PHYSICAL REVIEW
LETTERS

VOLUME 73 | 31 OCTOBER 1994 | NUMBER 18

Construction of Invariant Tori and Integrable Hamiltonians

Mikko Kaasalainen* and James Binney
Theoretical Physics, Keble Road, Oxford OX1 3NP, England
(Received 25 February 1994)

We present a general nonperturbative method for constructing an integrable Hamiltonian that is close to a given nonintegrable one. The existing invariant tori of the original Hamiltonian are accurately approximated by the constructed one. We illustrate the method by applying it to apparently near-integrable gravitational potentials for which no underlying integrable Hamiltonians are known.

PACS numbers: 03.20.+i, 05.45.+b, 95.10.Fh, 95.75.Pq

The computation of the invariant phase-space tori of Hamiltonian systems is an important problem in many fields ranging from plasma physics [1] and semiclassical quantum theory [2] to stellar dynamics [3] and accelerator physics [4]. Several schemes for the computation of these invariant tori have been developed. Traditionally, invariant tori have been constructed perturbatively. This approach, which culminated in the Kolmogorov-Arnold-Moser theorem, is limited by the tendency of tori to change their topology abruptly as the underlying dynamical problem is changed: These abrupt changes make the required deformation of a torus inherently nonanalytic and undermine the convergence of perturbative series. Consequently, most problems must be handled nonperturbatively.

Recently [4–6], techniques have been developed for nonperturbatively determining the generating function of a canonical transformation that maps the invariant tori of an integrable Hamiltonian into approximately invariant tori of a given Hamiltonian. Approaches, such as these, that are based on generating functions can be argued to be inherently superior [5] to ones that directly construct approximate invariant tori. However, in their simplest form [4,5] they are liable to break down when the given Hamiltonian is very far from any known integrable one. The method described here overcomes these difficulties by augmenting the generating function's canonical transformation with a point transformation. We also describe how approximate invariant tori constructed on a grid of values of the actions enable one to fit an integrable Hamiltonian to any given one in such a way that any invariant tori of the given Hamiltonian are also invariant tori of the fitted Hamiltonian.

Tailor-made action-angle coordinates.—In our scheme, invariant tori in the phase space of a known integrable "toy" Hamiltonian H_T are mapped to the phase space of a given "target" Hamiltonian H; we employ the convention that primed variables relate to the tori of H, while the unprimed ones correspond to those of H_T. The transformation between the ordinary phase-space coordinates $(\mathbf{x},\mathbf{p})$ and the action-angle coordinates $(\mathbf{J},\boldsymbol{\theta})$ of H_T is known. Our final product is an integrable Hamiltonian $H_0(\mathbf{J}')$ that closely approximates H and shares with H whatever invariant tori H may possess.

The scheme consists of three basic steps [5–8]: (i) construct tori, labeled by actions $\mathbf{J}'$, that are approximate invariant tori of H, (ii) construct consistent angle coordinates θ' for the created tori, and (iii) generalize steps (i) and (ii) for values of $\mathbf{J}'$ that do not correspond to invariant tori of H.

We illustrate our approach by applying it to the logarithmic potential

$$\Phi(x,y) = \frac{1}{2}\ln\left(x^2 + \frac{y^2}{q^2} + R_c^2\right), \qquad (1)$$

where $R_c = 0.14$ and q is varied in the range $(0,1]$. This represents a nonaxisymmetric planar gravitational potential, such as that of an elongated galaxy [9]. A typical $(x,\dot{x})$ surface of section is shown in Fig. 1. Orbits belonging to two major orbit families dominate Fig. 1:

0031-9007/94/73(18)/2377(5)$06.00

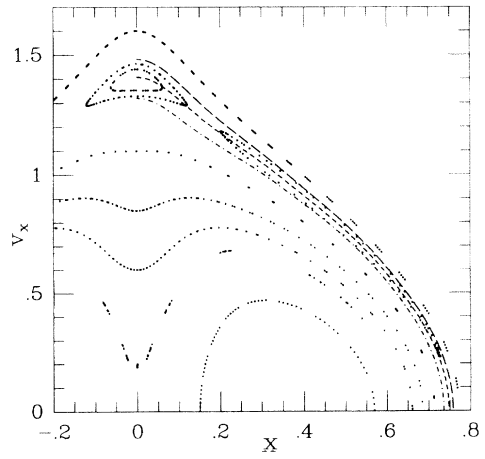

FIG. 1. $(x,\dot{x})$ section for the logarithmic potential (1) with $q = 0.8$ at $H = -0.199$. Dots are integrated consequents, and the dashed lines are curves of numerically constructed tori.

those that have a constant sense of circulation around the origin ("loops") and those that have not ("boxes"); their invariant curves circulate around $(x,\dot{x}) \simeq (0.4,0)$ and $(0,0)$, respectively. Similar orbits are supported by potentials whose Hamilton-Jacobi equations separate—the so-called Stäckel potentials [9,10]. A third, minor, family of orbits generates the pair of islands that is apparent toward the edge of the surface of section. These orbits may be considered to be trapped by a 2:3 resonance in a perturbed Stäckel potential. As q is decreased from unity, and the potential becomes more elongated, more and more of the phase space is occupied by similar minor families, whose members appear to be trapped by resonances [11].

By mapping the tori of a Stäckel potential, one could, in principle, recover the invariant tori of both major orbit families from a single toy Hamiltonian H_T. However, since analytic expressions are not available for the angle variables of Stäckel tori, it is more convenient to obtain the box and loop tori as images of the tori of two different toy Hamiltonians, whose orbits topologically resemble boxes and loops; we stress the fact that quantitatively they need not resemble H closely. Specifically, we obtain box tori from the two-dimensional harmonic oscillator and loop tori from the isochrone Hamiltonian

$$H_I = \frac{1}{2}\left(p_r^2 + \frac{p_\varphi^2}{r^2}\right) - \frac{k}{b + \sqrt{b^2 + (r - r_0)^2}}, \qquad (2)$$

where k, b, and r_0 are parameters and (r,φ) are planar polar coordinates.

In the simplest version of our scheme [5], we seek a generating function $S(\boldsymbol{\theta},\mathbf{J}')$ of the form

$$S(\boldsymbol{\theta},\mathbf{J}') = \boldsymbol{\theta}\cdot\mathbf{J}' - i\sum_{\mathbf{n}\neq 0} S_{\mathbf{n}}(\mathbf{J}')\exp(i\mathbf{n}\cdot\boldsymbol{\theta}), \qquad (3)$$

that directly maps the tori of H_T into those of H_0. The toy and target actions and angles are related by

$$\mathbf{J} = \partial S(\boldsymbol{\theta},\mathbf{J}')/\partial\boldsymbol{\theta}, \qquad \boldsymbol{\theta}' = \partial S(\boldsymbol{\theta},\mathbf{J}')/\partial\mathbf{J}'. \qquad (4)$$

The Levenberg-Marquardt algorithm is used to find the coefficients $S_{\mathbf{n}}$ that minimize the variation of H over the trial torus of given $\mathbf{J}'$. If H has an invariant torus $\mathbf{J}'$, H will be constant on the final torus to within the errors. The parameters k, b, r_0, etc., that define the toy potential are optimized together with the $S_{\mathbf{n}}$.

Generating functions of the type (3) are insufficiently general for many problems, and before mapping a toy torus with such a generating function, it must first be distorted by an appropriate point transformation [6]

$$\mathbf{x} \leftrightarrow \mathbf{x}', \qquad p_i' = \frac{\partial \mathbf{x}}{\partial \mathbf{x}_i'}\cdot\mathbf{p}. \qquad (5)$$

This transformation is designed to distort the toy orbit into the same general shape as the target orbit. In particular, it should map closed toy orbits into closed target orbits [6,12]. The tori of minor families can be obtained by mapping around a closed orbit an H_T that produces circulating or liberating motion. The less the motion in the toy potential resembles that in the target potential, the more important is the point transformation. For example, the box tori of Fig. 1 were obtained by mapping a Cartesian grid into the coordinate grid of confocal elliptic coordinates—this mapping distorts the rectangular box orbits of the harmonic oscillator into the butterfly shapes characteristic of box orbits in (1) [6]. The parameters describing the transformations are simultaneously optimized with the toy potential parameters and $S_{\mathbf{n}}$.

With this procedure one can produce, for any actions $\mathbf{J}'$, a torus of any specified type—box, loop, or resonant family [6,12]. Only certain tori will be useful, however. These are (a) those on which H is effectively constant, and (b) those which fill in an orderly way a region of phase space within which orbits are either chaotic or members of a minor family which is conveniently treated as comprising resonantly trapped orbits. The three dashed curves in Fig. 1 show an example of the latter phenomenon; they show sections of three box-orbit tori which effectively bound and slice through the islands of the 2:3 resonant family. The entire island zone can be filled by similar least-squares fitted tori. Of course, these are not invariant tori of H, which here differs significantly from the integrable Hamiltonian H_0 for which they are invariant tori. The value of H_0 on any fitted torus is defined to be the average value of H on that torus.

It is instructive to compare our scheme for constructing invariant tori with that of Warnock [4]. The latter employs a generating function of the form (3) but determines the $S_{\mathbf{n}}$ by numerically integrating an orbit from appropriate initial conditions, evaluating $(\mathbf{J},\boldsymbol{\theta})$ along the orbit, and then solving for the values taken by $\mathbf{J}$ on a regular grid in $\boldsymbol{\theta}$; the values of $\mathbf{n}S_{\mathbf{n}}$ and $\mathbf{J}'$ then follow from the

first equation of (4) on discrete Fourier transformations. This scheme is less general than ours in that (a) it can only yield tori that are invariant tori of H, and (b) it is only applicable if the toy and target tori are fairly similar. When applicable, it is more accurate, however, since with it there is no practical objection to employing all the $S_{\mathbf{n}}$ with $|\mathbf{n}| < N$ (typically, $N \simeq 30$), whereas in our scheme computational tractability demands that one set to zero as many of the $S_{\mathbf{n}}$ as possible. In view of this superior accuracy, it is advantageous to combine our scheme with that of [4]: Our scheme is first used to optimize a point transformation and the toy potential parameters and determine a crude generating function. Then Warnock's scheme is used to refine the generating function with the other parameters taken as optimized. As an example of this approach in action, in Fig. 2 we compare fits to five tori in the potential (1) with $q = 0.9$. Resonant islands in this surface of section are too small to be visible, so the Hamiltonian is Stäckel-like. The dashed curves show sections of tori obtained by least-squares fitting, while the solid lines show tori constructed by Warnock's method using the toy potential and point transformation parameters returned by the least-squares fits. The computational effort is approximately the same in both techniques for comparable resolution [13].

To complete the target action-angle coordinate system, by Eq. (4) one must determine the derivatives $\partial S_{\mathbf{n}}/\partial \mathbf{J}'$ of the coefficients $S_{\mathbf{n}}$ derived above. These derivatives are required at constant values of the parameters defining H_T and any point transformation. Since we *do* vary these parameters from orbit to orbit, we have to provide a mechanism for determining, torus by torus, the $\partial S_{\mathbf{n}}/\partial \mathbf{J}'$ we would obtain if we did calculate S for fixed parameters.

A convenient method [6] is numerically to integrate the orbit from initial conditions chosen to lie on the torus $\mathbf{J}'$ and substitute into the second equation of (4) the values $\boldsymbol{\theta}(t)$ taken by the toy angle variables along each orbit section. For the corresponding values of the target angle variables we substitute

$$\boldsymbol{\theta}' = \boldsymbol{\theta}'_0 + \boldsymbol{\omega}' t , \tag{6}$$

where $\boldsymbol{\theta}'_0$ is an unknown initial phase and $\boldsymbol{\omega}'$ is the orbital frequency vector. This yields a linear system of equations for the coefficients $\partial S_{\mathbf{n}}/\partial \mathbf{J}'$, the initial phases $\boldsymbol{\theta}'_0$, and $\boldsymbol{\omega}'$. Figure 3(a) shows the trajectories in toy-angle space of 36 orbit integrations started from different points on the torus corresponding to the uppermost box orbit of Fig. 2. Figure 3(b) shows the same trajectories in target-angle space. The dots in Figs. 3(a) and 3(b) show the input and output angles $\boldsymbol{\theta}$ and $\boldsymbol{\theta}'$, respectively, and the straight lines in Fig. 3(b) show the associated trajectories (6).

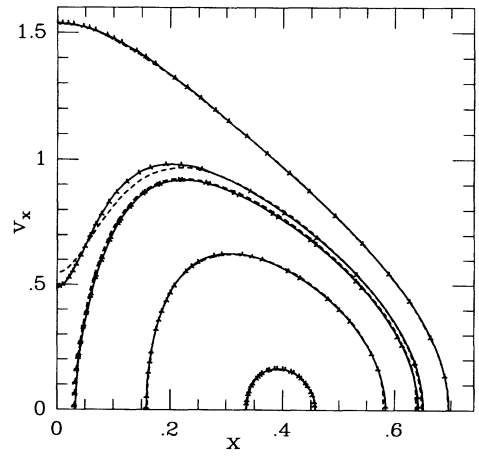

FIG. 2. $(x, \dot{x})$ at $q = 0.9$ and $H = -0.315$. The points show consequents obtained by direct orbit integration, and the lines are the invariant curves obtained by two torus construction algorithms.

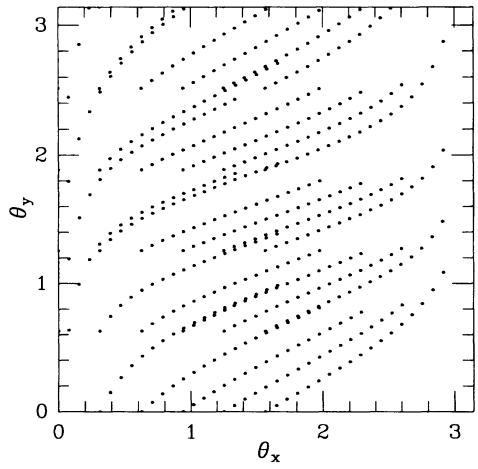

(a)

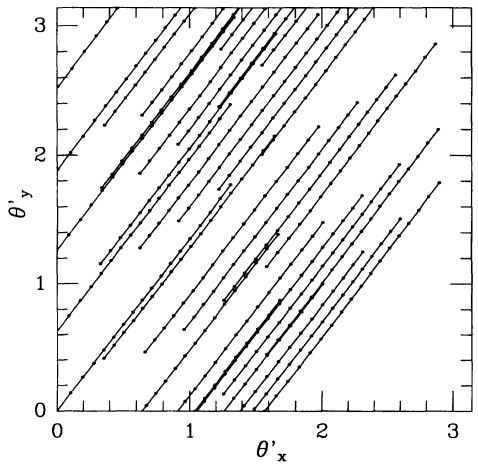

(b)

FIG. 3. (a) Trajectories in toy angle space obtained by direct integration of the equations of motion from 36 starting points on the uppermost torus of Fig. 2. (b) The same trajectories in target angle space (dots), together with the semianalytical linear trajectories (6) (straight lines).

Defining H_0 and applying perturbation theory.—Once tori have been constructed and furnished with angle variables and frequencies for a grid of $\mathbf{J}'$ values, it is a simple matter to define an integrable Hamiltonian H_0 for which these are invariant tori. The value of H_0 on the created tori that approximate existing invariant tori of H is defined to be the average value of H (i.e., $H_0 = H$ in principle). By interpolating smoothly in $\mathbf{J}'$ between the tori, we obtain all the quantities needed to define a torus for any given $\mathbf{J}'$ [8] (also, cf. [14]). Since we are in a position to specify at each grid point not only the function H_0 but its gradients $\boldsymbol{\omega}' = \partial H_0/\partial \mathbf{J}'$ as well, the chosen interpolation scheme for H_0 should utilize all these values consistently.

We define tori for values of $\mathbf{J}'$ that lie between the grid points by independently interpolating the $S_\mathbf{n}$, the $\partial S_\mathbf{n}/\partial \mathbf{J}'$, and the variable parameters $\mathbf{P}$ in H_T and any point transformation—since the derivatives $\partial S_\mathbf{n}/\partial \mathbf{J}'$ are at constant values of the parameters, while the $S_\mathbf{n}$ correspond to varying values of the parameters, the former must be obtained by explicit interpolation rather than by differencing the latter. [Of course, if the parameters $\mathbf{P}$ are kept fixed, S and its derivatives must be interpolated self-consistently, not independently—when approximating an existing invariant torus of H, simply differencing an interpolated S will usually not produce derivatives that are consistent with (6), especially if the $\mathbf{J}'$ grid is not dense.]

To understand how separate interpolations can be consistent, write $S_\mathbf{n} = S_\mathbf{n}(\mathbf{J}', \mathbf{P}(\mathbf{J}'))$. Then have

$$\frac{dS_\mathbf{n}}{d\mathbf{J}'} = \left(\frac{\partial S_\mathbf{n}}{\partial \mathbf{J}'}\right)_\mathbf{P} + \left(\frac{\partial S_\mathbf{n}}{\partial \mathbf{P}}\right)_{\mathbf{J}'} \cdot \left(\frac{\partial \mathbf{P}}{\partial \mathbf{J}'}\right). \tag{7}$$

When $\partial \mathbf{P}/\partial \mathbf{J}'$ is nonzero, there should be many acceptable solutions for $\partial S_\mathbf{n}/\partial \mathbf{P}$ that fulfill consistency between the $S_\mathbf{n}$ and their total derivatives (7). The actual solutions are not needed; it is sufficient to know that they can be constructed.

With these definitions the phase-space point $(\mathbf{x}, \mathbf{p})$ corresponding to given $(\mathbf{J}', \boldsymbol{\theta}')$ is immediately computable. Combining this with the definition of $H_0(\mathbf{J}')$ given above completes the definition of the integrable Hamiltonian $H_0(\mathbf{x}, \mathbf{p})$.

Given this procedure for constructing an integrable Hamiltonian that is close to any near-integrable one, it is natural to view the given Hamiltonian as a perturbation of the constructed one by writing

$$H(\mathbf{J}', \boldsymbol{\theta}') = H_0(\mathbf{J}') + \delta H(\mathbf{J}', \boldsymbol{\theta}'). \tag{8}$$

Standard secular perturbation theory [15] requires slight modification [8], however, because δH often effectively vanishes through much of phase space, whereas the standard theory assumes that δH is significant also far from trapping resonances. Also, δH is sometimes more asymmetric in $\mathbf{J}'$ than assumed in the standard theory. Figure 4 shows an example of how well a minor family can be represented as orbits resonantly trapped by δH.

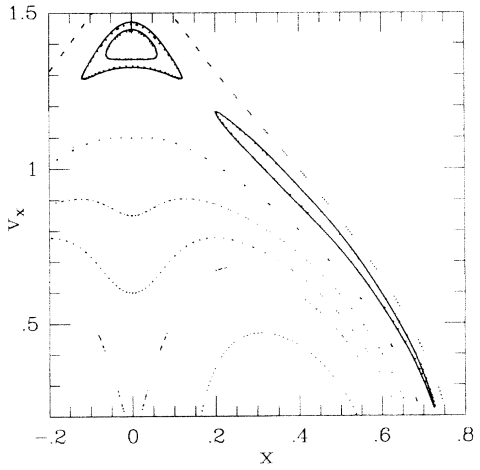

FIG. 4. A surface of section as in Fig. 1 (the v_x scale has been slightly expanded); the solid curves show islands obtained by perturbing the numerically constructed Hamiltonian $H_0(\mathbf{J}')$.

In conclusion, techniques have now been developed that enable one to construct an integrable Hamiltonian H_0 that closely fits any given Hamiltonian H. The orbits of most nontrivial Hamiltonians fall into several distinct families. For each significant family, one seeks a combination of a point transformation and a generating function (3) that maps the invariant tori of a toy Hamiltonian into approximately invariant tori of H. After fitting tori to every family one wishes H_0 to possess, a torus through an arbitrary point in phase space can be found by interpolation in the quantities which define the fitted tori.

Although results are presented here only for systems with $d = 2$ degrees of freedom, the methods are immediately generalizable to larger values of d. The computational cost rises steeply with d, however. We estimate that three-dimensional problems will require a few hundred times more CPU cycles than two-dimensional ones. The latter require usually only a minute or so for one torus on an average workstation. Hence this machinery should facilitate dynamical studies over a wide range of physical problems.

*Present address: NORDITA, Blegdamsvej 17, Copenhagen 2100, Denmark.

[1] A. H. Boozer, Phys. Fluids **25**, 520 (1982); Princeton Technical Report No. PPPL-2082, 1984.
[2] C. C. Martens and G. S. Ezra, J. Chem. Phys. **86**, 279 (1987).
[3] J. J. Binney and D. Spergel, Mon. Not. R. Astron. Soc. **206**, 159 (1984).
[4] R. Warnock, Phys. Rev. Lett. **66**, 1803 (1991).
[5] C. McGill and J. J. Binney, Mon. Not. R. Astron. Soc. **244**, 634 (1990).
[6] M. Kaasalainen and J. J. Binney, Mon. Not. R. Astron. Soc. **268**, 1033 (1994).
[7] J. J. Binney and S. Kumar, Mon. Not. R. Astron. Soc. **261**, 584 (1993).

[8] M. Kaasalainen, Mon. Not. R. Astron. Soc. **268**, 1041 (1994).
[9] J. J. Binney and S. Tremaine, *Galactic Dynamics* (Princeton University Press, Princeton, N.J., 1987).
[10] P. T. de Zeeuw, Mon. Not. R. Astron. Soc. **216**, 273 (1985).
[11] J. Miralda and M. Schwarzschild, Astrophys. J. **339**, 752 (1989).
[12] M. Kaasalainen and J. J. Binney, in Proceedings for Integration Algorithms for Classical Mechanics, Waterloo, 1993 (unpublished).
[13] In cases of potentials like (1), the computational cost is significantly reduced when one uses the symmetries of the corresponding Hamiltonian [5,6]. To be able to employ the symmetries, we use a grid with an even number of points in a dimension. Because of this, the matrix element D_{jk} in Eq. (5) of [4] is multiplied by $\cos[\pi(x_j - k)/K]$ in our case (K being even).
[14] R. Warnock and R. Ruth, Phys. Rev. Lett. **66**, 990 (1991); Physica (Amsterdam) **56D**, 188 (1992).
[15] A. Lichtenberg and M. Lieberman, *Regular and Stochastic Motion* (Springer, New York, 1993).